Earthquake Engineering, Tenth World Conference © 1992 Balkema, Rotterdam. ISBN 90 5410 060 5

Behavior of composite columns under seismic conditions

James M. Ricles & Shannon A. Paboojian
University of California, San Diego, Calif., USA

ABSTRACT: An experimental study was undertaken to investigate the cyclic strength and ductility of composite columns subjected to simulated seismic loading conditions. Six two-thirds scale specimens were tested, each consisting of a structural steel shape encased in reinforced concrete. Parameters studied in the test program included the degree of concrete confinement required to achieve adequate ductility, effectiveness of shear studs for developing flexural stiffness and capacity under combined loading, and distribution of transverse shear resistance among the elements of the composite column. The results of the test program indicate that composite columns possess exceptional ductility and strength under cyclic loading if the buckling of longitudinal reinforcement is inhibited. Furthermore, the steel shape provides the primarily resistance to transverse shear during overloading, and shear studs are not effective in enhancing the resistance against lateral loading.

1 INTRODUCTION

The use of composite construction in nonseismic structural systems has been recognized in the United States as a viable means of designing and constructing buildings. For the construction of exterior parameter moment resisting frames in tall buildings, it is feasible to erect a steel frame using wide flange shapes and then to encase the steel columns in reinforced concrete to complete the structure. The permanent placement of the steel frame allows it to be used both as an erection frame during construction and as part of the structural system upon completion of construction, thereby expediting the construction process. From a structural point of view, the composite frame possesses the structural characteristics of inherent stiffness of reinforced concrete, and the strength, longspan capability, and lightweight properties of structural steel. A composite frame is designed on the premise that the steel shape be capable of resisting construction dead load, often up to ten floors, and the composite columns be capable of resisting additional gravity loading and lateral loading.

The benefits of composite construction make it appealing for use also in seismic zones. However, there currently exist a lack of knowledge about the behavior of encased composite columns under severe cyclic seismic loading. Although seismic design guidelines are currently being formulated in the U.S. for composite columns [NEHRP, 1994] there is a lack of experimental results to provide a basis for recommending design details that ensure adequate cyclic strength and ductility. An experimental research program was therefore undertaken at the University of California, San Diego to investigate the cyclic strength and ductility of structural steel wide flange shapes (W-shapes) encased in reinforced concrete. Issues that were studied included: lateral stiffness; transverse shear resistance; degree of concrete confinement to achieve good ductility; and effectiveness of shear studs in resisting lateral loading. Reported herein is a summary of the results of six tests involving the application of combined axial, flexural, and shear loading. A complete report of the test program can be found in reference 5 [Ricles et al, 1992].

2 TEST PROGRAM

Test specimens were designed which represented a two-thirds scale model of a ground floor column in an exterior 30 to 40 story composite moment resisting frame. The axial (P), shear (V), and flexural (M) forces developed in the column under combined gravity and lateral seismic loading were determined and used to design the specimens. Ductility corresponding to coordinates on a axial load-moment (P-M) interaction surface were calculated for a composite column similar to the specimens tested in order to determine acceptable levels of imposed axial load P relative to the member's capacity. This involved modeling the cross section as a

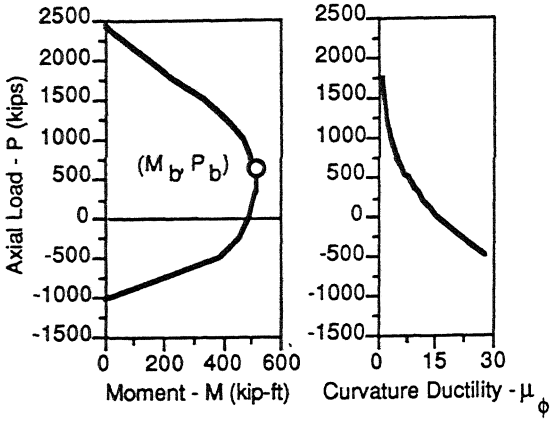

Figure 1. Moment-axial load interaction surface for composite column (Specimen 3).

media of discrete fibers, each fiber possessing its own material characteristics corresponding to either steel or concrete, and assuming that plane sections remain plane, with full strain compatibility between steel and concrete fibers (e.g. full composite action). The results of the analysis are shown in Figure 1, where the P-M interaction surface has been placed along side a plot of the curvature ductility μ_ϕ corresponding to the level of axial load on the P-M interaction surface. The curvature ductility is defined as $\mu_\phi = \phi_u / \phi_y$, where ϕ_u, ϕ_y = curvature corresponding to initial yield of extreme tensile longitudinal reinforcement, and curvature at a compressive strain of $\varepsilon_u = 0.016$ in the extreme concrete fibers, respectively.

It is apparent from Figure 1 that it is desirable to design composite columns for an axial load below the member's balance axial load P_b, at which the extreme tensile longitudinal reinforcement develops its yield strain while the concrete extreme fibers simultaneously develop their ultimate compressive strain. For axial loads below P_b there is a notable increase in ductility and hence energy dissipation if lateral loading causes overloading. Each specimen was therefore designed on the basis that its resistance was such that the applied axial load of 335 kips (1490 KN) corresponded to $0.8P_b$, with the P-M interaction surface based on full strain compatibility and ACI criteria for concrete (e.g. $\varepsilon_u = 0.003$).

Four cross sectional details were tested: Details A, B, C, and D (see Figure 2). Detail A consist of twelve - longitudinal steel reinforcement bars, with a closed No. 3 rectangular tie supplemented by a closed No. 3 octagon shaped tie for additional confinement. Detail B omitted the octagon tie, and used four corner longitudinal bars. Detail C was similar to Detail A, as was Detail D being similar to Detail B, except for the addition of 0.5 in. (1.27 cm.) diameter by 2 in. (5 cm.) long steel shear studs spaced at 7.5 in. (19 cm.) on each flange of the W-shape. The spacing of the shear studs was determined on the basis that shear studs combined with a 320 psi (2.21 MPa) bond stress, acting on the outside compressive flange surface, be capable of transferring to the W-shape the concrete compressive resultant associated with the design point on the P-M interaction surface.

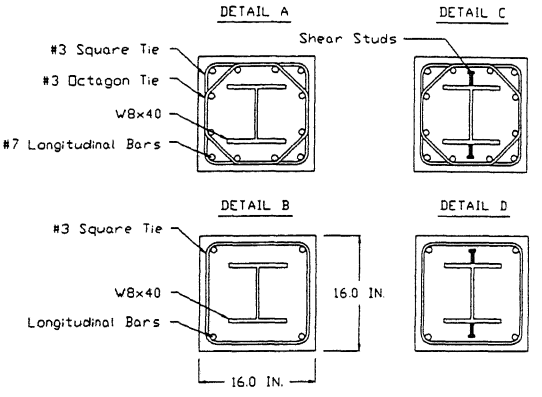

Figure 2. Specimen details (1 in = 2.54 cm).

A summary of the general details for each specimen is given in Table 1, where d_b, A_s, A_g, s, and L = bar diameter and total area of longitudinal steel reinforcement, gross area of specimen, tie spacing along lower 32 in. (81.3 cm.) height of specimen, and shear span of specimen, respectively. In the upper part of each specimen, away from the base where the plastic region forms in the column under lateral load, a rectangular tie spaced at 5 in. (12.7 cm.) was used. Each specimen had a W8x40 steel shape encased in reinforced concrete, which amounted to 4.5% of the column's gross area A_g. The W8x40 had a measured yield stress of 54 ksi (372.3 MPa), with the longitudinal bars an average yield stress of 63 ksi (434.4 MPa). The concrete compressive strengths were 4.98 ksi (34.3 MPa), 4.45 ksi (30.7 MPa), and 5.11 ksi (35.2 MPa) for Specimens 1 and 2, 3 and 4, 5 and 6, respectively. A base plate was welded to the bottom of each W8x40. In Specimens 1 and 2 it was partially submerged into the column's footing, where the top of the plate was flush with the top surface of the footing. For all of the other specimens, the base plate was totally submerged 10 in. (25.4 cm.) below the top surface of the footing. The base plate of all specimens was anchored using 6 - 1 in. (2.54 cm.) diameter A490 bolts, which were secured into the footing using an uplift plate as a mechanical anchor at the end of the

bolts. In Specimens 1 and 2 the base plate was post tensioned to the footing by tightening the bolts after curing of the concrete had taken place.

Table 1 Specimen details

Spec No.	d_b (in)	$\frac{A_S}{A_g}$	s (in)	L (in)	Detail Type	s_{max} (in)
1	0.875	0.019	5.0	98	A	4.1
2	1.375	0.023	2.5	98	B	6.5
3	0.875	0.028	3.75	76	A	4.1
4	1.125	0.016	3.75	76	B	5.3
5	0.875	0.028	3.75	76	C	4.1
6	1.125	0.016	3.75	76	D	5.3

1 in. = 2.54 cm.

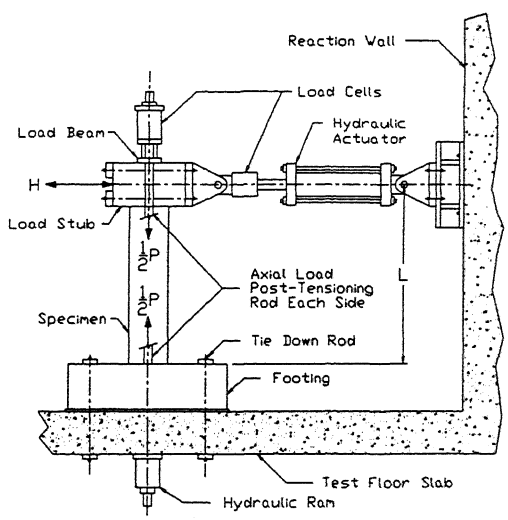

Figure 3. Test setup.

The test setup shown in Figure 3 was used to test each specimen under combined axial load P and lateral load H. A specimen was secured in place by post tensioning its footing to the test floor. The height L of the specimen corresponded to the distance from the base to the point of inflection in the prototype column. Each specimen was tested by applying the 335 kips (1490 KN) of axial gravity load P, through the use of two post tensioning rods and a load beam placed over the top of the specimen. The lateral force H, simulating the seismic loading, was then cyclically applied under displacement control, using a hydraulic actuator placed at the height of L above the base of the column. The amplitude of displacement Δ was equivalent to μ = 0.2, 0.4, 0.6, 0.8, 1.0, 1.5, 2.0, 3.0, 4.0,... in successive sets of cycles. A set constituted three symmetric cycles of displacement, where $\mu = \Delta/\Delta_y$ and Δ_y = displacement at nominal flexural capacity M_{ACI} corresponding to full composite action with strain capability [ACI, 1989]. The ensuing forces developed in the column near the base included axial, shear, and flexural, and simulated the combined force state developed in a ground floor column during an earthquake. Each specimen was extensively instrumented for displacements, curvature, strains, and applied loads.

3 TEST RESULTS

The horizontal top displacement-load relationship (hysteresis loops) for Specimens 1 and 3 are shown in Figure 4(a) and (b). Specimen 1 developed yielding of its longitudinal reinforcement at the base of the column at μ = 0.75, followed by flange yielding near μ = 2.0. At μ = 4.0 the outer core of concrete, between the ties and outside face of the specimen, spalled at the base of the column. Continued cyclic loading resulted in the buckling of the No. 7 longitudinal reinforcement, where s= 5 in. (12.7 cm.), just above the base at μ = 5.3. This led to the deterioration of the inner core of concrete and a loss of capacity. The maximum moment developed in Specimen 1 was M_{max}=5538 k-in. (625.7 KN-m), occurring near μ = 2.0. Specimen 3 responded with tension reinforcement yielding at μ = 0.75, followed by flange yielding at μ = 1.75 and outer core spalling at μ = 4.0. Unlike Specimen 1, Specimen 3 did not suffer bar buckling and consequently showed no signs of deterioration. At a displacement corresponding to μ = 6.0 the test was stopped, having reached the limit of the actuator stroke. For Specimen 3, M_{max}=6942 k-in. (784.4 KN-m), and was developed initially in the cycle with an amplitude of μ = 2.0, and reached in all subsequent cycles. The performance of Specimen 3 is considered exceptional, for it dissipated energy in a stable manner and showed no signs of deterioration in capacity (the spacing s of the ties was equal to 3.75 in.). It would be expected that a severe earthquake could impose a ductility demand corresponding to μ = 4.0. To assure that a member is adequate it should be able to achieve μ = 6.0 in an experimental test program without a significant loss of load carrying capacity.

Values for maximum ductilities, μ_{max}, and flexural moments M_{max} for each specimen are summarized in Table 2. Specimen 2's ductility was limited to μ_{max} = 4.3 due to a fracture of the base plate to W-shape fillet weld connection. However, prior to the fracture the specimen showed no signs of deterioration, which is attributed to the good confinement provided by the tie spacing of s=2.5 in. (6.35 cm.). Specimen 4 reached μ_{max} = 5.0 before a tie at the base of the column showed signs of bulging outwards under the confining pressure, between the

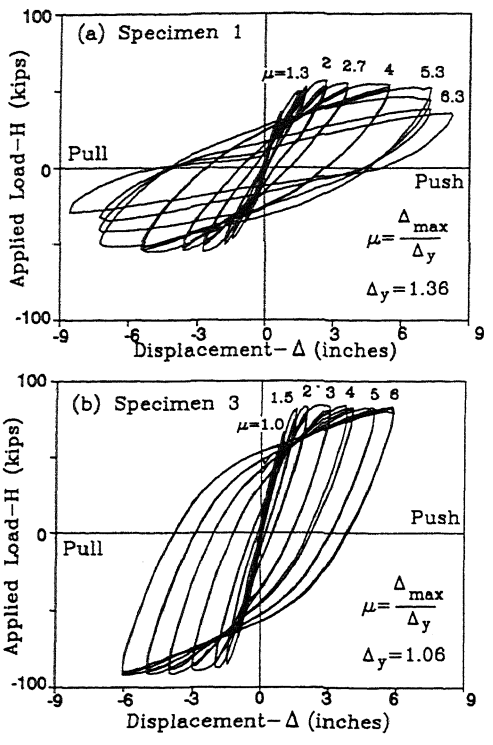

Figure 4. Hysteretic response for Specimens 1 and 3 (1 in = 2.54 cm, 1 kip = 4.448 KN).

corner longitudinal bars, and eventually opened up. This caused buckling of the longitudinal bars and a deterioration of the concrete core surrounding the W8x40, leading to a rapid deterioration in specimen load carrying capacity.

Table 2 Specimen Capacity and Comparison with Strength Predictions.

Spec. No.	Experimental		Exper./Analytical		
	μ_{max}	M_{max} (k-in)	$\frac{M_{max}}{M_{ACI}}$	$\frac{M_{max}}{M_{LRFD}}$	$\frac{M_{max}}{M_{SRC}}$
1	5.3	5538	1.16	1.34	1.05
2	4.3	5246	1.22	1.43	1.11
3	6.0	6942	1.23	1.34	1.13
4	5.0	5934	1.20	1.32	1.08
5	6.0	6868	1.22	1.33	1.13
6	6.4	5904	1.19	1.31	1.06

1 k-in = 0.113 KN-m

Specimen 5, being similar to Specimen 3 with the addition of shear studs, was able to develop a ductility of μ = 6.0. After a cycle at this ductility, the tensile No. 7 longitudinal reinforcement bars began to fracture, leading to their buckling and loss of concrete core upon load reversal. The maximum moment of M_{max} = 6868 k-in. (776 KN-m) developed in Specimen 5 was almost equal to that of Specimen 3, M_{max} = 6942 k-in. (784.4 KN-m). Specimen 6, which also had shear studs, achieved μ = 6.4 before longitudinal bar buckling occurred due to the bulging of the ties between corner longitudinal bars, which lead to a deterioration of the concrete core, W-shape flange buckling, and a loss of load carrying capacity. The maximum moment developed in Specimen 6 was M_{max} = 5904 k-in. (667.1 KN-m), and nearly equal to that of Specimen 4, M_{max} = 5934 k-in. (670.5 KN-m).

4 ASSESSMENT OF TEST RESULTS

A comparison of M_{max} with capacity M_{ACI} predicted by the ACI Code [ACI, 1989] based on full composite action with strain compatibility, and capacity M_{LRFD} based on LRFD provisions for nonseismic composite columns [AISC,1986], are given in Table 2. Included in Table 2 is also a comparison with the capacity M_{SRC} which is based on superimposing the individual P-M interaction surfaces of the W-shape and the reinforced concrete. This procedure is similar to that currently used in Japan for composite structures [AIJ, 1987]. It is apparent in Table 2 that the superimposed strength method is most accurate (an average of 9.5% below M_{max}), while the ACI method gives an average of 20% below M_{max} and the LRFD method 35% below M_{max}. The average increase in capacity M_{max} of 20% above M_{ACI} is attributed to the large neutral axis depth in the composite column, which leads to a flexural strength more dependent on the concrete contribution and a greater effect of confinement. The ACI provisions do not account for any increase in concrete strength due to confinement. The LRFD predicted strength being rather low relative to M_{max} is attributed to the inaccuracy of LRFD to predict column strength when the composite column has a small steel shape.

The envelop of the hysteresis loops, corresponding to the first cycle at each level of ductility, are shown in Figure 5 for Specimens 3 and 5. It can be seen that the results for these specimens are practically identical. The same was found for Specimens 4 and 6 (not shown). It is apparent that the shear studs do not effectively increase the elastic and cracked stiffness, nor the lateral load capacity. The capacity of the cross section of Specimen 3 and 5 was predicted to be H_u = 88.2 kips (392.3 KN), based on a *fiber analysis assuming full composite action*, and is marked in Figure 5. Figure 5 indicates that this full composite action capacity H_u is developed in the specimens, and that shear studs are not necessary to achieve this. An assessment of the lateral stiffness preceding

yielding at H = 66 kips (293.6 KN) indicates that using a section stiffness based on $0.5E_cI_g$ gives a good prediction of displacement up to reinforcement yielding (see Figure 5), where E_c, I_g = concrete Young's modulus, and moment of inertia based on gross cross section properties. The use of E_cI_g, which is currently being considered for adoption [NEHRP, 1994] in design for elastic analysis to determine load effects and required strength, will tend to underestimate deflections. It should be noted that the above phenomena associated with the effectiveness of shear studs and stiffness were also observed when comparing the behavior of Specimens 4 and 6 (not shown).

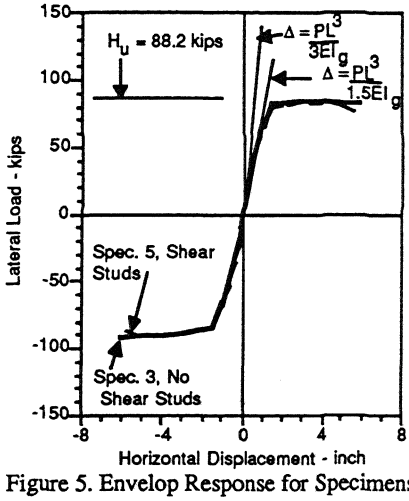

Figure 5. Envelop Response for Specimens 3 and 5.

Strains measured on the web of the W-shape, by means of strain rosettes, and in the ties, using strain gages, were used to determine the distribution of shear among the W-shape (V_S), transverse ties (T), and concrete (V_C). The measured strains of the web and ties were converted to stresses, and integrated across the material of the cross section. The conversion in the inelastic range required the use of incremental plasticity theory. The Von Mises yield criterion for metals, together with the assumption of no work hardening was adopted. By assuming that the total measured applied shear H was equal to $V_S + T + V_C$, the unknown resistance of V_C could then be determined. Figure 6(a) and (b) show for Specimens 1 and 3 the shear resistance as a function of ductility. It is apparent that the concrete is initially responsible for resisting almost all of the applied shear until the concrete shear capacity V_{CAP} is reached, after which the resistance V_C deteriorates as the W-shape resists a large portion of the applied shear. The capacity of V_{CAP} was found to correlate well with that

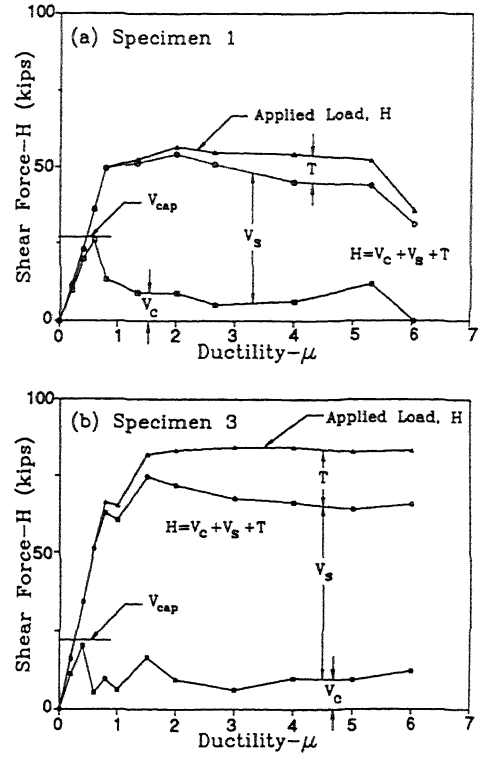

Figure 6. Transverse shear resistance for Specimens 1 and 3 (1 kip = 4.448 KN).

based on the ACI provisions [1989] for reinforced concrete, considering the portion of the concrete in the cross section outside the wide flange to only be effective in resisting shear. The resistance of V_S supplied by the W-shape is seen in Figure 6 to reach a maximum in the range of μ = 1.5 to 2.0, corresponding to flange yielding, after which a small redistribution takes place between the W-shape and the transverse ties, T. It appears that the effectiveness of the transverse ties in resisting transverse shear is limited by the shear deformability of the W-shape, for the measured tie strains were found to be less than half their yield strain.

The behavior of the specimens implies that the buckling of the longitudinal bars must be inhibited in order to maintain the concrete core and achieve adequate ductility. This can be accomplished by a proper tie spacing, in addition to providing sufficient tie stiffness in the region of the member where major inelastic behavior is expected. Tie stiffness is achieved by supplying steel tie area A_{sh} at a spacing of s and limiting the clear distance between longitudinal reinforcement. An evaluation of the specimen details indicated that A_{sh} based on New Zealand criteria [1982] for reinforced concrete was adequate where:

$$A_{sh} \geq 0.3\, s\, h \left(\frac{A_g}{A_c} - 1 \right) \frac{f'_c}{f_{yh}} \left(0.5 + 1.25 \frac{P}{f'_c A_g} \right) \quad (1)$$

and

$$A_{sh} \geq 0.12\, s\, h \frac{f'_c}{f_{yh}} \left(0.5 + 1.25 \frac{P}{f'_c A_g} \right) \quad (2)$$

in which all terms are defined in reference 6 [New Zealand, 1982]. To inhibit longitudinal buckling the maximum tie spacing s should satisfy:

$$s \leq \frac{d_b}{4} \sqrt{\frac{\pi^2 E_r}{f_y}} \quad (3)$$

where d_b, f_y, and E_r = longitudinal reinforcement diameter, yield stress, and reduced Young's modulus, respectively. E_r is determined using reduced modulus theory applied to inelastic buckling of a reinforcement bar, where it can be shown for a circular bar:

$$E_r = \frac{4EE_t}{(\sqrt{E} + \sqrt{E_t})^2} = 0.08E \quad (4)$$

In Equation (4) E and E_t = elastic Young's modulus, and Young's modulus at the onset of strain hardening of the steel reinforcement. Substituting Equation (4) into (3), with E = 29000 ksi (200 GPa) and f_y = 63 ksi (434.4 MPa), the maximum tie spacing s_{max} should be

$$s_{max} = 4.75 d_b \quad (5)$$

Values for s_{max} related to the test specimens were calculated, and are tabulated in Table 1. Only Specimen 1's tie spacing exceeded s_{max}, which suffered bar buckling. Although longitudinal bar buckling was also observed in some specimens having a tie spacing less than s_{max}, these specimens had a displacement ductility close to μ = 6.0 (with the exception of Specimen 2 which had a base plate connection failure) and used either Detail B or D. Details B and D are not as effective as Details A and C, for the former have too large of clear spacing of longitudinal bars along the tie, which results in less effective concrete core confinement and longitudinal bar restraint by the tie.

5 CONCLUSIONS

Based on the test results reported herein, the following conclusions are noted:

1) Cyclic strength and ductility in composite columns under severe cyclic loading is dependent on confinement of the concrete surrounding the structural steel shape. Longitudinal bar buckling must be prevented to preserve the integrity of the member. A maximum closed tie spacing of 4.75 longitudinal bar diameters is suggested.

2) The flexural strengths predicted by the several codes are conservative. The strength superposition, based on the P-M interaction surfaces, appears to be the most accurate for estimating composite column capacity.

3) The design of composite columns for shear should be based on the concrete being required to resist all shear at service load levels (μ< 0.75), and the W-shape resist all shear under seismic loading conditions.

4) Shear studs in composite columns are neither effective nor required to develop lateral stiffness and flexural capacity.

5) Welded based plate details perform better if they are submerged into the footing, where they are not exposed to as high of curvature.

REFERENCES

ACI Committee 318. 1989. "Building Code Requirements for Reinforced Concrete (ACI 318-89)," *American Concrete Institute*, Detroit, Michigan.

American Institute of Steel Construction. 1986. "Load and Resistance Factor Design," *Manual of Steel Construction*, AISC Inc., Chicago, Illinois.

Architectural Institute of Japan . 1987. "AIJ Standards for Structural Calculation of Steel Reinforced Concrete Structures."

National Earthquake Hazards Reduction Program. 1994. " Recommended Provisions for the Development of Seismic Regulations for New Buildings", *Draft*, Building Seismic Safety Council, Washington, D.C.

Ricles, J., Paboojian, S., and Bruin, W. 1992. "Experimental Study of Composite Columns Subjected to Seismic Loading Conditions," *Report*, Structural Systems Research Project, University of California, San Diego.

Standard Association of New Zealand. 1982. "Design of Concrete Structures: New Zealand Standard 3101," Wellington, New Zealand.

ACKNOWLEDGEMENTS

The research program reported herein was supported by the Engineering Foundation and the National Science Foundation. The opinions expressed in this paper are those of the authors and do not necessarily reflect those of the sponsors. The authors would like to thank Bill Bruin and Chris Hodge, undergraduate assistants in the Department of AMES, who provided valuable effort in constructing specimens, testing, and reducing data.